



Originally published as:

Sørensen, M. B., Stromeyer, D., Grünthal, G. (2010): Attenuation of macroseismic intensity in the Campania region, S Italy. - *Journal of Seismology*, 14, 2, 209-223

DOI: [10.1007/s10950-009-9162-2](https://doi.org/10.1007/s10950-009-9162-2)

# Intensity attenuation in the Campania region, Southern Italy

M. B. Sorensen • D. Stromeyer • G. Grünthal

Received: 13 March 2008 / Accepted: 26 March 2009  
© Springer Science + Business Media B.V. 2009

**Abstract** Ground motion prediction equations (GMPE) in terms of macroseismic intensity are a prerequisite for intensity-based shake maps and seismic hazard assessment and have the advantage of direct relation to earthquake damage and good data availability also for historical events. In this study, we derive GMPE for macroseismic intensity for the Campania region in southern Italy. This region is highly exposed to the seismic hazard related to the high seismicity with moderate- to large-magnitude earthquakes in the Apenninic belt. The relations are based on physical considerations and are easy to implement for the user. The uncertainties in earthquake source parameters are accounted for through a Monte Carlo approach and results are compared to those obtained through a standard regression scheme. One relation takes into account the finite dimensions of the fault plane and describes the site intensity as a function of Joyner–Boore distance. Additionally, a relation describing the intensity as a function of epicentral distance is derived for implementation in cases where the dimensions of the fault plane are unknown. The relations are based

on an extensive dataset of macroseismic intensities for large earthquakes in the Campania region and are valid in the magnitude range  $M_w = 6.3$ – $7.0$  for shallow crustal earthquakes. Results indicate that the uncertainties in earthquake source parameters are negligible in comparison to the spread in the intensity data. The GMPE provide a good overall fit to historical earthquakes in the region and can provide the intensities for a future earthquake within 1 intensity unit.

**Keywords** Macroseismic intensity • Attenuation • Ground motion prediction • Campania region • Intensity data points • Earthquake early warning • Seismic hazard

## Abbreviations

PGA Peak ground acceleration  
IDP Intensity data point  
GMPE Ground motion prediction equation

## 1 Introduction

The Campania region in southern Italy is highly exposed to the seismic hazard related to the high seismicity with moderate-to large-magnitude earthquakes in the Apenninic belt. Most recently, the destructive  $M_w = 6.9$  Irpinia earthquake in 1980 caused more than 3,000 casualties

---

M. B. Sorensen (✉) • D. Stromeyer • G. Grünthal  
GFZ German Research Centre of Geosciences,  
Section 2.6 Seismic Hazard and Stress Field,  
Telegrafenberg, 14473 Potsdam, Germany  
e-mail: sorensen@gfz-potsdam.de

as well as widespread serious damage to buildings and infrastructures throughout the region, underlining the crucial importance of seismic hazard and risk assessment in the region. One measure in this direction is the efforts towards the implementation of an earthquake early warning system (Weber et al. 2007). Most critical in this respect is the city of Naples, which has a population reaching two million.

When generating shake maps as part of an earthquake early warning system, an essential parameter is the attenuation of seismic waves in the area of interest. Such information is also crucial in seismic hazard assessment. Modern ground motion prediction equations (GMPE) are typically given in terms of recorded ground motion parameters, for example peak ground acceleration (PGA) based on strong motion data. When studying the damage potential of large earthquakes, such PGA-based relations have two drawbacks. First, the availability of recordings is limited and therefore one is often forced to apply GMPE based on recordings from different areas with similar tectonics. Second, there is no straightforward way to associate the recorded ground motions with damage, which is a complex function of ground motion level, ground shaking duration, local site conditions, and building vulnerability. This also implies that direct conversion from recorded ground motion (such as PGA) to intensity is associated with large scatter.

As an alternative, to overcome these problems, ground motion attenuation can be expressed in terms of macroseismic intensity. Intensities have the major advantage of good data availability, as

data are dependent on the availability of people and a built environment rather than instrumentation and therefore can be sampled closer and as far back in time as historical records allow. Especially for the Italian territory, a very complete and extensive dataset of macroseismic intensities is available. Furthermore, the macroseismic intensity is assigned based on the observed ground shaking or damage, and thereby, it can be directly related to the damage potential of future earthquakes. Another advantage is that intensity data are easily understandable by non-seismologists and easily convertible by risk management teams.

Several previous studies have focused on the issue of macroseismic intensity attenuation in Italy (Albarello and D'Amico 2004; Berardi et al. 1993; Faccioli and Cauzzi 2006; Gasperini 2001; Gómez 2006). The GMPE presented in these studies are listed in Table 1. Additionally, Sponheuer (1960) derived special parameters for his relation for selected earthquakes in the Apennines. Most of the existing models are given as a function of the epicentral intensity,  $I_0$ , and some distance measure to the earthquake source. Berardi et al. (1993) and Gómez (2006) represent the intensity attenuation as proportional to the cubic root of epicentral distance. Gasperini (2001), on the other hand, concludes that a bilinear attenuation function of epicentral distance provides the best fit to the observed intensities. Albarello and D'Amico (2004) derive a relation including both a linear and a logarithmic term for the hypocentral distance. All authors provide average relations for the whole Italian territory, whereas Gómez (2006) provides three additional relations valid for nor-

**Table 1** Intensity prediction equations for Italy

	Author	Relation
	Berardi et al. (1993)	$I = I_0 + 0.729 - 1.122 \times R_{epi}^{1/3}$
	Gasperini (2001)	$I = I_0 - 0.52 - 0.056 \times R_{epi}$ ( $R_{epi} \leq 45\text{km}$ ) $I = I_0 - 0.52 - 0.056 \times 45 - 0.0217 \times (R_{epi} - 45)$ ( $R_{epi} > 45\text{km}$ )
	Albarello and D'Amico (2004)	$I = 3.6 - 0.003 \times R_h - 0.98 \times \ln(R_h) + 0.705 \times I_0$
	Gómez (2006)	$I = I_0 + 1.3096 - 1.1833 \times R_{epi}^{1/3}$
	Faccioli and Cauzzi (2006)	$I = 1.0157 + 1.2566 \times M_w - 0.6547 \times \ln\left(\sqrt{R_{JB}^2 + 2^2}\right)$

$I_0$  epicentral intensity,  
 $R_{epi}$  epicentral distance,  
 $R_h$  hypocentral distance,  
 $M_w$  moment magnitude,  
 $R_{JB}$  Joyner–Boore distance

mal fault mechanisms, reverse and strike-slip mechanisms and the Etna area, respectively. This is in line with comments included by all authors that regional variations are present in the attenuation pattern in Italy. The only study based on magnitude instead of epicentral intensity is that of Faccioli and Cauzzi (2006) who derive a relation based on mainly Italian earthquakes, supplemented with significant events in the Mediterranean region.

In the current study, we present local GMPE valid for the Campania region in southern Italy. One model takes into account the finite extent of the fault plane and represents the site intensities as a function of Joyner–Boore distance and moment magnitude. The other model describes attenuation as a function of epicentral distance for implementation in, e.g., early warning systems or seismic hazard analyses in cases where details of the fault parameters are not known for all earthquakes in a catalog. In order to test the effect of uncertainties in the earthquake source parameters, we derive the relations using an innovative Monte Carlo approach and compare to the results of a standard regression technique. As basis for the relations, we use the extensive dataset of the DBMI04 database (Stucchi et al. 2007), which is the most recent database of macroseismic intensities for Italy.

## 2 Method

The regressions for GMPE for macroseismic intensity are based on the least-squares regression method of Stromeyer and Grünthal (2009) for the well-established and physically based attenuation model for point sources (Sponheuer 1960):

$$I = I_0 - a \times \log \sqrt{\frac{R^2 + h^2}{h^2}} - b \times (\sqrt{R^2 + h^2} - h). \quad (1)$$

In this expression,  $I_0$  is the epicentral intensity,  $R$  is epicentral distance, and  $h$  is focal depth, usually taken as the hypocenter depth. The first term,

$a \times \log \sqrt{\frac{R^2 + h^2}{h^2}}$ , describes the geometrical spreading (having its main effect at short distances) and the second term,  $b \times (\sqrt{R^2 + h^2} - h)$ , represents the energy absorption (most significant at larger distances). The original form of Eq. 1 goes back to Kövesligethy (1906) and Jánosi (1907) on the basis of an empirical relationship between intensity and peak ground acceleration established by Cancani (1904).

$I_0$  represents the intensity of ground shaking at the epicenter and provides the link between Eq. 1 and the strength of the earthquake. It can be replaced by any magnitude- and depth-dependent relation,  $I_0 = I_0(M, h)$ . Here, we use a regression model between  $I_0$ , moment magnitude  $M_w$ , and depth  $h$  (Stromeyer et al. 2004):

$$I = c \times M_w + d \times \log(h) + e. \quad (2)$$

Assuming all input data to be known, Eqs. 1 and 2 define a linear regression problem for the five parameters  $a$ ,  $b$ ,  $c$ ,  $d$ , and  $e$ . In the current implementation, however, the depths of most of the studied earthquakes are not known. To overcome this problem, we replace  $h$  in Eqs. 1 and 2 by an “average depth” parameter  $h^*$  representing a characteristic depth in the region, which is determined as an additional regression parameter.

In this way, our model becomes nonlinear:

$$I = c \times M_w + e^* - a \times \log \sqrt{\frac{R^2 + h^{*2}}{h^{*2}}} - b \times (\sqrt{R^2 + h^{*2}} - h^*). \quad (3)$$

The parameter  $e^*$  replaces the term  $d \times \log(h) + e$  in 2, as its single components cannot be separated when the individual event depths are not known.

Equation 3 is in many respects comparable with the common type of strong-motion prediction equations (e.g., Joyner and Boore 1993). For large earthquakes, the point source assumption fails and the finiteness of the fault must be accounted for. We choose to include the finite dimensions of the fault by defining the distance  $R$  as the Joyner-Boore distance, i.e., the shortest

distance to the surface projection of the rupturing fault plane. In this respect, a GMPE is derived, which is symmetric around the surface projection of the rupturing fault plane.

Input data for the regression is a collection of intensity data points (IDP) describing the observed intensity at a given location. To avoid bias due to variation in the number of observations for different intensity classes, a weighting scheme is applied where each intensity class (half or integer intensity level) is assigned the same weight in the regression regardless of the number of observations within the class. Therefore, the determination of the regression parameters  $a$ ,  $b$ ,  $c$ ,  $e^*$ ,  $h^*$  leads to the weighted least-squares problem:

$$\min_x \left\| W^{-1}(I - A(x)) \right\| \quad (4)$$

where  $I = (I_i)$ ,  $i = 1, \dots, n$ , is a vector of  $n$  IDP,  $A$  describes the nonlinear attenuation model,  $W$  is an  $(n \times n)$  weighting matrix with only diagonal entries, and  $x = (c, e^*, a, b, h^*)$  is the parameter vector to be estimated. The values of the diagonal elements of  $W$  are chosen in such a way that (1) they are equal for all data in one intensity class and (2) the sum of squared inverse weights is equal for all intensity classes (classes are identically weighted). This defines the weights up to an arbitrary constant scaling factor which does not influence the regression solution  $x$  but is important for estimating uncertainties for a new intensity predicted by the model. The natural way of rescaling  $W$  is such that the mean weighted and unweighted residuals are equal:

$$W_{\text{new}} = W_{\text{old}} \frac{\left\| W_{\text{old}}^{-1}(I - A(x)) \right\|}{\left\| I - A(x) \right\|}. \quad (5)$$

The uncertainties in the estimated parameters  $x$  and in predicting a new intensity  $I$  for given predictor values  $M_w$  and  $R$  are connected with the covariance matrix  $C$  of the parameter estimates and the mean squared regression error:

$$\sigma^2 = \frac{\left\| I - A(x) \right\|^2}{n - m} \quad (6)$$

where  $m$  is the dimension of  $x$  (the number of model parameters). For a specified level of certainty  $\alpha$ , the confidence bounds  $x^c$  for the fitted parameters  $x$  are given by:

$$x^c = x \pm t^{-1}((1 - \alpha)/2, n - m) \cdot \sqrt{\text{diag}(C)} \quad (7)$$

where  $t^{-1}(p, \nu)$  is the inverse of the cumulative  $t$ -distribution for the corresponding probability  $p$  and  $\nu$  degrees of freedom. For  $\nu \geq 40$ ,  $t^{-1}(p, \nu) \approx N^{-1}(p)$ , the inverse of the cumulative standard normal distribution at  $p$ . In this case, a certainty level of 68.3% ( $\alpha = 0.683$ ) corresponds to the standard deviation ( $1\sigma$ ) of normally distributed errors.

Much more interesting in this study is the error of a new intensity prediction  $I$  of the estimated model. For given predictor values  $M_w$  and  $R$ , this can be expressed by:

$$I_{\text{error}} = t^{-1}((1 - \alpha)/2, n - m) \times \sqrt{\sigma^2 + y^T C y} \quad (8)$$

where  $y$  is the Jacobian of Eq. 3 with respect to the model parameters at the predictor values:

$$y^T = \frac{\partial A}{\partial x} = \left( M_w, 1, -\log \sqrt{\frac{R^2 + h^{*2}}{h^{*2}}}, -\left( \sqrt{R^2 + h^{*2}} - h^* \right), \frac{\partial A}{\partial h^*} \right). \quad (9)$$

### 3 Data

As input to our analysis, we have extracted macroseismic intensity data from the DBMI04 database (Stucchi et al. 2007). As our main focus is on the city of Naples, we have included earthquakes which were felt here with  $I \geq 6$ . Only events with a minimum of 30 intensity observations are included. We focus our study on events occurring in the Apenninic belt or at shorter distance to Naples to avoid influence of different tectonic environments. These criteria lead to the selection of nine earthquakes, which are listed in Table 2. Event locations are shown in Fig. 1.

When extracting data from the DBMI04 database, only IDPs which have been assigned a numerical intensity value have been included, leav-

**Table 2** Earthquakes providing data for the intensity prediction equations

Year	Date	$M_w^a$	$I_{\min}^b$	$I_{\max}^b$	$I_0^b$	#IDP
1456	5 Dec	7.0	5	11	10	197
1688	5 Jun	6.7	5	11	11	169
1694	8 Sep	6.9	3	11	10.5	244
1702	14 Mar	6.3	4	10	9.5	31
1732	29 Nov	6.6	5	10.5	10.5	167
1805	26 July	6.6	4	10	10	207
1857	16 Dec	7.0	2	11	10.5	311
1930	23 July	6.4 <sup>c</sup>	2	10	10	498
1980	23 Nov	6.9	2	10	10	1,161

$M_w$  moment magnitude,  $I_{\min}$  minimum observed intensity,  $I_{\max}$  maximum observed intensity,  $I_0$  epicentral intensity, #IDP number of intensity observations

<sup>a</sup> From CPTI04 catalogue (Gruppo di lavoro CPTI 2004)

<sup>b</sup> From DBMI04 database (Stucchi et al. 2007)

<sup>c</sup> From Emolo et al. (2004)

ing out data points classified as, for example, “felt”. Points which have been assigned an uncertain intensity value (e.g., 7–8, which means that the data can be interpreted equally well as intensity 7 or 8) were given the intermediate half-integer value (e.g., 7–8 was given the value 7.5). It should be noted here that this practice, implying a not existing accuracy, is generally not recommendable (see, e.g., Grünthal 1998 for details), but we find it necessary as intensities must be entered as numerical values in the regression and

excluding the “double-intensity” points (7–8 in our example) would lead to a significant reduction of the dataset. Furthermore, visual inspection indicates that the half-integer intensities follow the distribution of integer intensities and thereby are not expected to introduce any bias in the derived GMPE. When interpreting intensity predictions from this study, we recommend considering non-integer intensity predictions in a similar manner by assigning predictions close to a half-integer value the corresponding “double intensity” value. Only very few sites have observed intensities smaller than 3, and we therefore define 3 as a lower intensity limit in our final dataset. The available intensity range, epicentral intensity, and the number of IDPs are listed for each event in Table 2. The number of observations in each intensity class for each earthquake is listed in Table 3.

In order to calculate the Joyner-Boore distance, it is necessary to determine the location of the fault plane for each earthquake. Instrumental recordings exist only for the 1930 and 1980 earthquakes, and for the remaining events, source parameters based on macroseismic intensity data have been used. As we are interested also in estimating the uncertainty in the derived relations, we provide the source parameters with an associated uncertainty. The source parameters and their uncertainties are listed in Table 4 and details are given in the following.

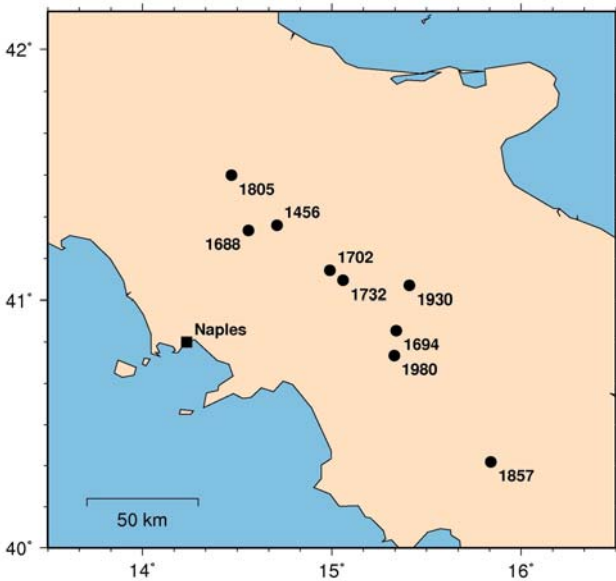


**Fig. 1** Locations of the nine earthquakes used in the regression analysis for intensity prediction equations.

**Table 3** Data distribution in terms of intensity values for the studied earthquakes

	Intensity																
	3	3.5	4	4.5	5	5.5	6	6.5	7	7.5	8	8.5	9	9.5	10	10.5	11
1456	–	–	–	–	1	–	28	3	22	6	35	18	64	8	9	–	3
1688	–	–	–	–	2	–	15	18	9	10	55	5	32	6	14	–	3
1694	3	3	–	–	4	1	2	20	71	14	50	19	21	5	15	15	1
1702	–	–	1	–	–	1	1	1	1	2	7	7	6	–	4	–	–
1732	–	–	–	–	4	–	1	7	2	90	25	13	11	10	2	2	–
1805	–	–	3	3	7	2	26	18	65	26	16	12	9	12	8	–	–
1857	2	–	15	4	26	–	42	44	51	29	53	12	8	3	16	–	2
1930	17	14	39	13	67	4	52	40	123	43	52	5	6	2	3	–	–
1980	107	30	309	35	230	10	188	26	136	2	55	–	9	–	6	–	–

Epicenter location, magnitude, strike, and dip for the 1930 and 1980 earthquakes are taken from the studies of Emolo et al. (2004) and Dziewonski et al. (1988), respectively. For the remaining events, except the one in 1456, source information is taken from Gasperini et al. (1999) who derive the epicenter location and strike of the fault plane based on the distribution of macroseismic intensities under the assumption that the macroseismic field represents the location and orientation of the rupturing fault. The 1456 event is not included by Gasperini et al. (1999) and the epicenter location is therefore taken from the CPTI04 catalogue (Gruppo di lavoro CPTI 2004)

which, for the other events, is consistent with the results of Gasperini et al. (1999). The strike of the 1456 event is taken as the average of three events with similar intensity distributions and assigned an uncertainty equal to the largest uncertainty associated with the three strikes. The location uncertainties for all epicenters are assumed to be 10 km as is claimed by Gasperini et al. (1999) to be typical for events in their database. Uncertainties in the strike orientations of the events are taken as listed by Gasperini et al. (1999). For the two most recent events, an uncertainty in the strike of  $15^\circ$  is assumed which is also observed as an appropriate value by Gasperini et al. (1999).

**Table 4** Source parameters for the studied earthquakes

Earthquake	Lon ( $^\circ$ E, km)	Lat ( $^\circ$ N, km)	$M_w^a$	Strike (deg)	Dip (deg)
1456 <sup>a</sup>	$14.71 \pm 10$	$41.30 \pm 10$	$7.0 \pm 0.3$	$125^b \pm 27$	$45^c \pm 30$
1688 <sup>d</sup>	$14.56 \pm 10$	$41.28 \pm 10$	$6.7 \pm 0.3$	$118 \pm 14$	$45^c \pm 30$
1694 <sup>d</sup>	$15.34 \pm 10$	$40.88 \pm 10$	$6.9 \pm 0.3$	$121 \pm 12$	$45^c \pm 30$
1702 <sup>d</sup>	$14.99 \pm 10$	$41.12 \pm 10$	$6.3 \pm 0.3$	$107 \pm 189$	$45^c \pm 30$
1732 <sup>d</sup>	$15.06 \pm 10$	$41.08 \pm 10$	$6.6 \pm 0.3$	$92 \pm 96$	$45^c \pm 30$
1805 <sup>d</sup>	$14.47 \pm 10$	$41.50 \pm 10$	$6.6 \pm 0.3$	$124 \pm 27$	$45^c \pm 30$
1857 <sup>d</sup>	$15.84 \pm 10$	$40.35 \pm 10$	$7.0 \pm 0.3$	$127 \pm 11$	$45^c \pm 30$
1930	$15.41^e \pm 10$	$41.06^e \pm 10$	$6.4^f \pm 0.3$	$110^f \pm 15$	$55^f \pm 15$
1980 <sup>g</sup>	$15.33 \pm 10$	$40.78 \pm 10$	$6.9 \pm 0.3$	$135 \pm 15$	$41 \pm 15$

Lon longitude, Lat latitude,  $M_w$  moment magnitude

<sup>a</sup> From CPTI04 catalogue (Gruppo di lavoro CPTI 2004)

<sup>b</sup> Average of 1694, 1805, and 1857 events which have similar intensity distributions

<sup>c</sup> Assumed following Gasperini et al. (1999)

<sup>d</sup> From Gasperini et al. (1999)

<sup>e</sup> Average of Kárník (1969), CNR-PFG (1985), Boschi et al. (1995), Oddone (1930) and the NEIS catalogue

<sup>f</sup> From Emolo et al. (2004)

<sup>g</sup> Dziewonski et al. (1988)

According to the CPTI04 catalogue, the errors associated with the moment magnitudes of the studied events are in the range 0.10–0.16. We find this estimate rather optimistic and choose to apply the error observed by Gasperini et al. (1999) of 0.3. There is no information available in the literature regarding the dip of the fault planes. As suggested by Gasperini et al. (1999), we assume a dip of  $45^\circ$  and associate it with a rather large uncertainty of  $30^\circ$  to reflect the lack of exact knowledge.

Based on the information in Table 4, the location of the fault plane is determined by assuming that the hypocenter is located in the center of the fault plane which is extended in the strike direction. This implies that the dip direction of the fault plane has no influence on the Joyner–Boore distance, as the surface projection of the fault plane is independent of dip direction. Fault dimensions are calculated from the relations of Wells and Coppersmith (1994) giving rupture length and rupture width as a function of moment magnitude for a general focal mechanism.

Not all the studied earthquakes have been presented with an estimate of the event depth, and the available depths are expected to be of varying quality. Postpischl (1985) presents a depth of 25–60 km for the 1732 event, 10 km for the event in

1805, and 5–25 km for the one in 1857. Emolo et al. (2004) found that the 1930 event occurred at a depth of less than 15 km, whereas Dziewonski et al. (1988) give a depth of 16 km for the 1980 event. It was attempted to derive the event depths through regression for each event, deriving a relation following Eq. 1, including the depth,  $h$ , as a parameter to be determined. However, the quality of data for most of the events is not sufficient for a stable single event regression. As we furthermore expect all earthquakes to be crustal, and within a limited depth range, it was decided to derive GMPE replacing the depth  $h$  by the “average depth” parameter  $h^*$  as described in the previous section. It should be emphasized that in cases where reliable depth information is available, inclusion of the actual event depths will lead to improved GMPE.

The final dataset consists of 2,945 IDP covering the intensity range 3–11 at distances of 0–660 km for earthquakes in the magnitude range  $M_w = 6.3$ –7.0. A plot of the distance ranges covered for each magnitude is presented in Fig. 2. From this figure, it is seen that distances more than 300 km are covered only by a single earthquake. Therefore, the final GMPE are valid in the aforementioned magnitude and intensity ranges for distances up to 300 km.

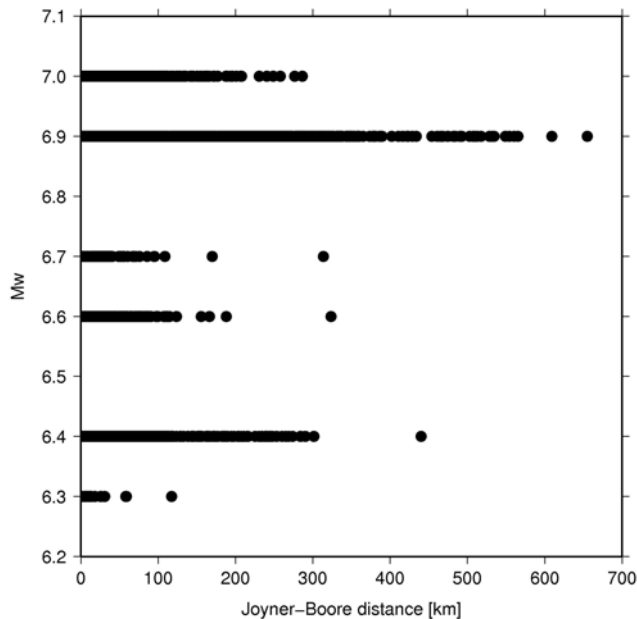


Fig. 2  $M_w$  vs. Joyner-Boore distance for the studied dataset

## 4 Results

In order to account for the uncertainties in all input parameters and get an estimate of the uncertainty in an intensity assignment, we derive the GMPE through a Monte Carlo approach, where we perform one million regressions with input parameters sampled within the uncertainty bounds defined for each parameter and compare to the results of a standard regression procedure. Location, magnitude, and strike were varied following a normal distribution with standard deviation equal to the uncertainties listed in Table 4. As we have little information about the dip of the fault planes, this parameter was sampled from a uniform distribution within the uncertainty bounds. The uncertainty related to deriving fault dimen-

**Table 5** Regression parameters and mean regression errors for Eq. (3)

Regression	c	e*	a	b	h*	$\sigma$
R <sub>JB</sub> (MC)	0.658	5.127	3.991	0.0012	10.761	0.948
R <sub>JB</sub> (Std)	0.986	3.151	3.309	0.0024	5.960	0.941
R <sub>epi</sub> (MC)	0.690	5.277	6.001	-0.0026	19.665	0.971
R <sub>epi</sub> (Std)	1.556	-0.428	5.518	-0.0020	15.550	0.972

MC Monte Carlo regression, Std standard regression

sions from the magnitude is not included, as this is already included through the variation in magnitude. For each realization, the distances were calculated and a regression for the parameters ( $a$ ,  $b$ ,  $c$ ,  $e^*$ ,  $h^*$ ) was made. Through this approach, the mean values of the parameters as well as their uncertainties were determined.

The obtained regression parameters for Joyner–Boore and epicentral distance are listed for the Monte Carlo (MC) approach and a standard nonlinear regression (Std) in Table 5. The individual regression parameters show some differences among the relations; however, this variation is to a large extent balanced in such a way that the intensities predicted by Monte Carlo-based relations are very similar to the ones from standard regressions, as is illustrated in Fig. 3.

The GMPE for epicentral distance are based on a point source assumption. Such models can be of

importance for early warning applications where source dimensions are not available in the first minutes after an earthquake and in seismic hazard analyses where the fault dimensions are not known for all events in an earthquake catalog. The similar quality of fit for the two distance measures is due to the intermediate magnitudes of the earthquakes implying relatively short fault lengths combined with the relatively shallow dip of the fault planes. These two factors in combination lead to isolines of Joyner–Boore distance which are close to circular, as are the isolines for epicentral distance. This means that the macroseismic fields derived from the two relations have similar shapes with slightly larger values of epicentral distance than for Joyner–Boore distance, as is also observed in Fig. 3. In applications for long steep-dipping faults (as is the case, for example, for the Marmara Sea region, see Sørensen et al. 2009), this is not the case, and the inclusion of the finite dimensions of the fault plane leads to a better fit of the observed intensity field.

The parameters  $b$  for epicentral distance in Table 5 are negative, indicating an increase of intensity with increasing distance for the energy absorption term. This can, of course, not be justified from a physical point of view and reflects the limitations in our dataset. It can be seen from Fig. 3 that for distances less than approximately 400 km, this increase is balanced by the anelastic attenuation term, and thereby, the relations provide correct intensity estimates within its validity bounds. For larger distances, the relations for epicentral distance predict unrealistically high intensities.

The ground shaking level is expected to decrease as a function of the distance to the fault plane rather than the distance to the epicenter, and

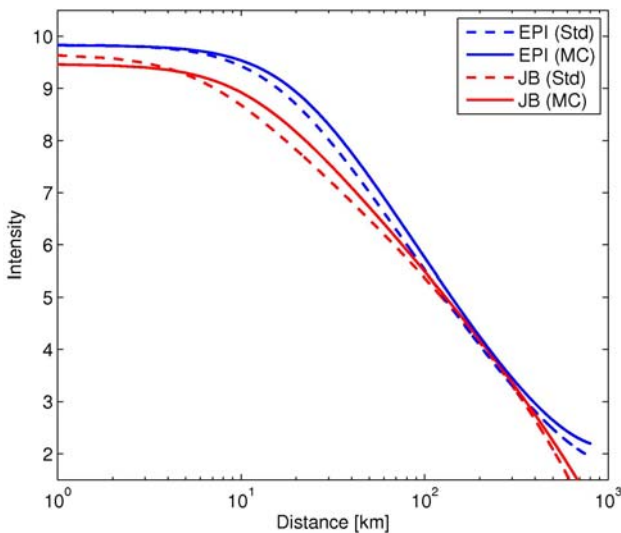


**Fig. 3** Comparison of the four intensity prediction equations for a  $M_w = 6.6$  earthquake. Solid lines indicate the Monte Carlo (MC) models, dotted lines are the standard regression (Std) results. EPI epicentral distance, JB Joyner–Boore distance

therefore, the relation based on Joyner–Boore distance is the most meaningful one from a physical point of view. However, in cases where Joyner–Boore distance cannot be calculated, it is better to use a relation derived based on epicentral distance than to simply use epicentral distance in a Joyner–Boore-distance-based relation. In this respect, the relation for epicentral distance is calculated for application purposes only and should, under no circumstances, be used for extrapolation outside the validity bounds.

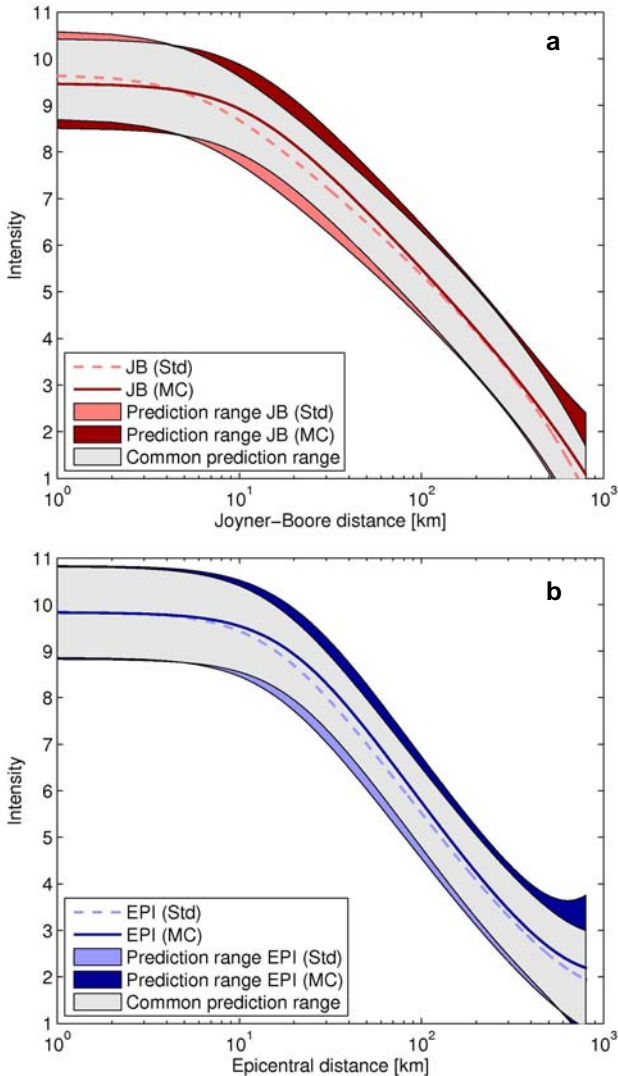


**Fig. 4** Comparison of prediction ranges for the Monte Carlo (MC) models and the standard regression (Std) results. The part of the prediction ranges which are common for the two models are marked as gray. **a** Joyner–Boore (JB) distance, **b** epicentral (EPI) distance

An interesting observation in Table 5 is that the mean regression errors obtained using the Monte Carlo approach are close to identical to the ones obtained through a standard regression. These regression errors indicate the level of uncertainty related to the intensity data. The error for a new intensity prediction depends additionally on the covariance matrix  $C$  of the fitted parameters  $x$  (Eq. 8), especially on the diagonal elements of  $C$  which are the squared uncertainties of  $x$ . As expected, these variances are considerably larger for the Monte Carlo regression than for the standard regression (for details, see the Appendix where the complete covariance matrices are listed). However, in both cases, the influence of the variance is small in comparison to the regression error. This is confirmed in Fig. 4 where the prediction ranges for the Monte Carlo approach and the standard regression are compared for the two distance measures. The consequence of this observation is that the uncertainties related to the earthquake location and source parameters have a negligible contribution to the errors in the derived relations. With the data currently available, macroseismic intensity in Italy can be predicted only within the range of approximately one intensity unit. In this respect, we see no necessity for propagating the uncertainties related to source parameters through regressions on intensity data which are characterized by an uncertainty of more than half an intensity unit.

As the four derived GMPE provide a comparable fit to the data, we show here only the performance of the relation derived for Joyner–Boore distance using the Monte Carlo approach. For each of the studied events, we present in Fig. 5 the observed intensities in comparison to the intensity predictions, including also the 68.3% prediction bounds. Here, we see that the uncertainties are to a large extent related to the spread in the observed data and that the average trend of the observations is well reproduced. The performance of the relation is also presented in terms of residuals (observed - predicted intensity) averaged over 5-km bins and their standard deviations vs. distance in Fig. 6. At distances of 50–350 km, where most intensity observations are available,

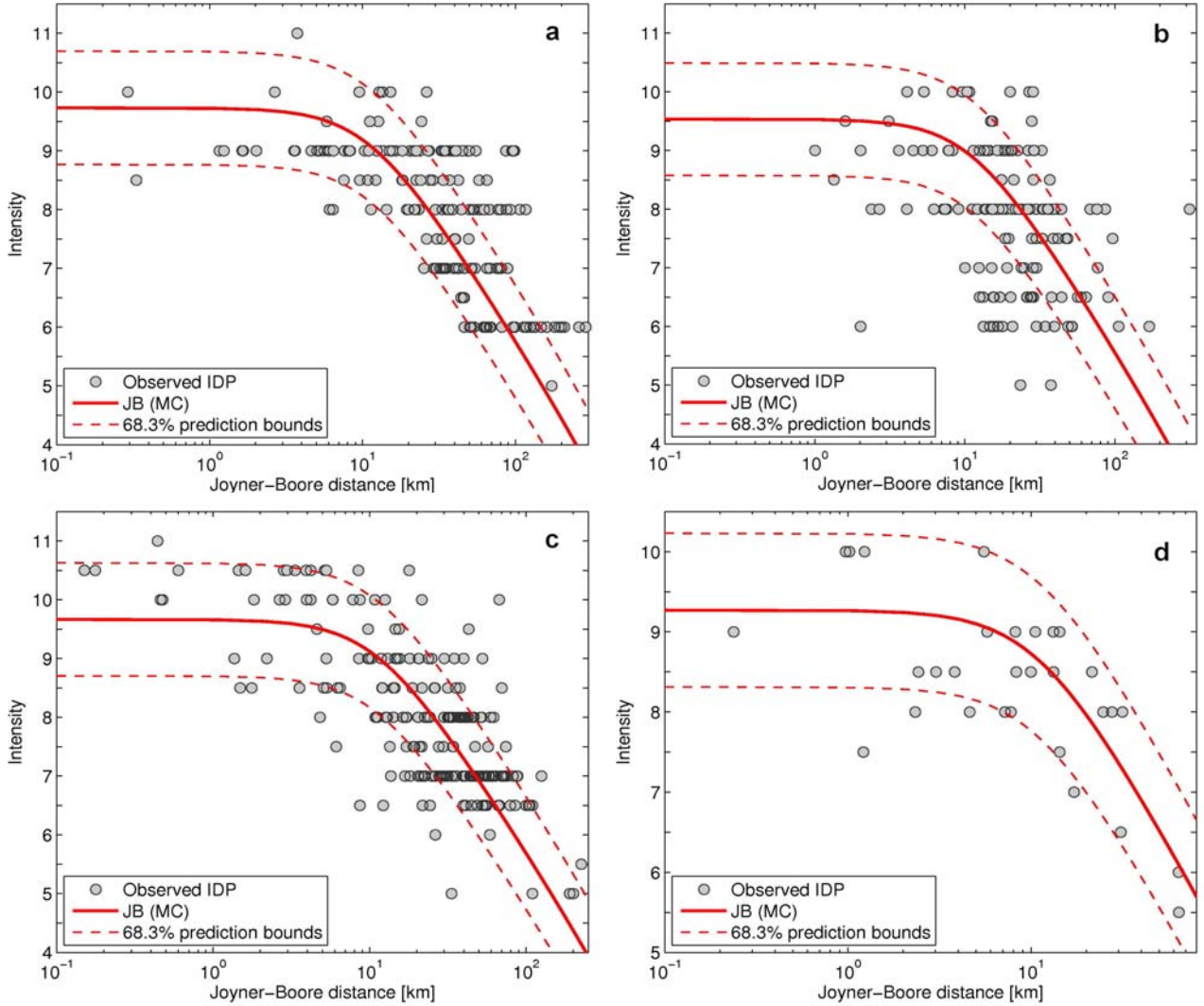


**Fig. 5** Intensity vs. distance plots comparing the observed intensities for the studied earthquakes (*circles*) with the intensities predicted from Eq. 3 for Joyner-Boore distance and the Monte Carlo approach (*solid red lines*). **a** 1456; **b** 1688; **c** 1694; **d** 1702; **e** 1732; **f** 1805; **g** 1857; **h** 1930; **i** 1980.

the mean residuals are small and scattered around 0. At shorter distances, our relation has a tendency to overestimate the intensities and, in this respect, represents a conservative estimate. However, the average residuals are smaller than the stated prediction error of approximately one intensity unit within the entire distance range.

In order to test how robust the attenuation model is, nine additional regressions were performed where the input events were left out one by one. The obtained regression parameters and associated regression errors are presented in Table 6. For the ten regressions (including the one for all events), the parameters  $a$  and  $b$ , which de-

scribe the decay of intensity with distance, are very similar. Also, the average depth parameter,  $h^*$ , does not vary much. On the other hand, there is some variation for the parameters  $c$  and  $e^*$  which describe the epicentral intensity as a function of magnitude. As these two parameters are determined from magnitudes within a relatively small magnitude range, they are expected to be much more sensitive to changes in the data. Plotting the intensity prediction as a function of distance for the ten relations (Fig. 7), however, shows that the obtained relations predict very similar intensity values, and thereby, the variation in  $c$  and  $e^*$  seems to be balanced for each relation.

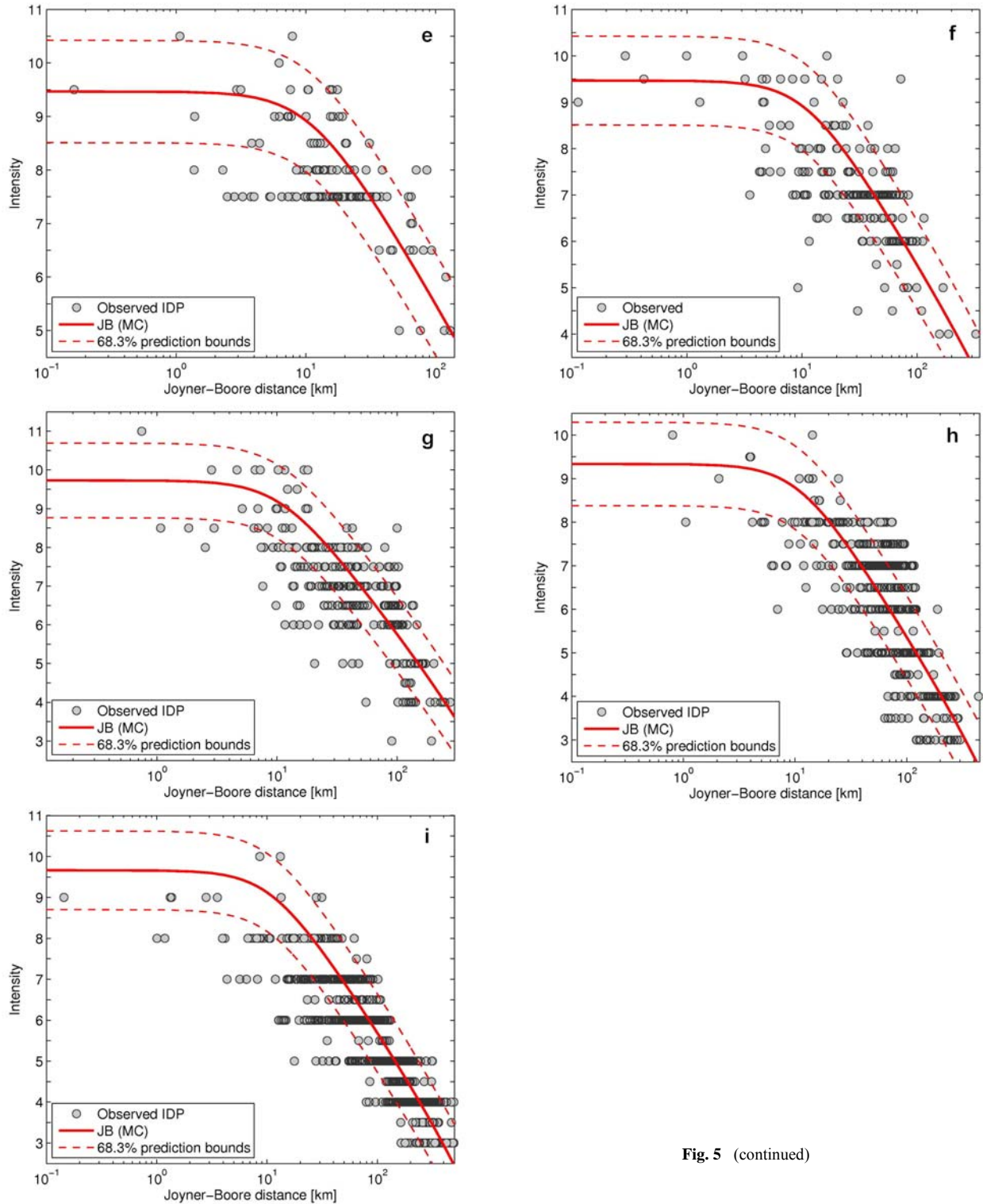
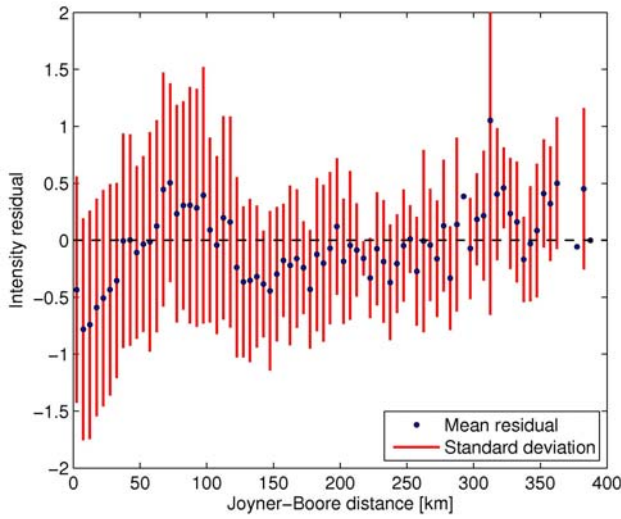


Fig. 5 (continued)

The two panels in Fig. 7 show intensity predictions for the lower and upper magnitude range of validity of our relations. As expected, the differ-

ence between the relations increases when extrapolating outside these ranges.

We compare our relations to the already exist-



**Fig. 6** Residuals (observed - predicted intensity) averaged over 5-km bins and associated standard deviations vs. distance. The comparison is made for the Monte Carlo based relation for Joyner-Boore distance.

ing intensity prediction equations for Italy, which are listed in Table 1. The comparison is based on the mean regression error for the single events (Eq. 6), taking into account the appropriate functional forms and number of parameters for the different models. The results are presented in Table 7. The comparison shows that all relations in general provide a similar quality fit to the data.

Our relations show stable low residuals, whereas other relations have very high residuals for some events. This may be due to our relations being based on data from all the considered earthquakes, whereas other relations can be based on different datasets. The similarity of fit for all relations with residuals of the order of one intensity

unit is in agreement with the observation that intensity predictions in Italy are necessarily limited within a one-intensity-unit range. The wide range of functional forms all give the possibility of fitting the data within this range and are as such equally valid for predicting ground motion intensities. The main strengths of our derived relations, in addition to being derived for local data from the Campania region, are twofold. Firstly, they have a physical basis and give the possibility of accounting for the finite dimensions of the fault plane. Secondly, all uncertainties are accounted for and the error related to a new intensity prediction is stated explicitly, giving the user the possibility of choosing a desired level of conservatism when applying the relations.

## 5 Conclusions

In the presented study, we have derived GMPE for macroseismic intensity for the Campania region in southern Italy. The relations are based on physical considerations and have a form which is straightforward to implement for the user. The uncertainties in earthquake location and fault parameters are accounted for in a Monte Carlo approach and results are compared to the results obtained with a standard regression technique. One relation takes into account the finite dimensions of the fault plane and presents the intensity as a function of Joyner-Boore distance, moment magnitude, and event depth. The other relation is

**Table 6** Regression parameters for Joyner-Boore distance obtained by excluding the events one by one for testing the robustness of the model

Regression	$c$	$e^*$	$a$	$b$	$h^*$	$\sigma$
All events	0.986	3.151	3.309	0.0024	5.960	0.941
Excluding 1456	0.780	4.523	3.353	0.0022	5.871	0.915
Excluding 1688	0.979	3.136	3.581	0.0017	7.197	0.925
Excluding 1694	0.914	3.545	3.430	0.0019	6.641	0.937
Excluding 1702	0.773	4.649	3.241	0.0026	5.549	0.939
Excluding 1732	1.051	2.706	3.313	0.0023	5.797	0.945
Excluding 1805	0.923	3.617	3.334	0.0027	6.073	0.942
Excluding 1857	1.251	1.371	3.172	0.0030	5.845	0.940
Excluding 1930	1.155	2.004	3.180	0.0027	5.415	0.909
Excluding 1980	1.010	3.045	3.226	0.0028	5.508	1.045

**Table 7** Comparison of average residuals for the nine earthquakes based on various intensity prediction equations for Italy

	1456	1688	1694	1702	1732	1805	1857	1930	1980
This study									
$R_{JB}$	1.180	1.253	0.932	0.860	0.930	0.981	1.018	1.081	0.755
$R_{JB}$ (Monte Carlo)	1.133	1.250	0.930	0.830	0.978	1.034	1.061	1.040	0.780
$R_{epi}$ (Monte Carlo)	1.311	1.206	1.000	0.889	1.030	1.053	1.003	0.996	0.827
Berardi et al. (1993)	1.899	1.110	1.155	1.296	0.709	0.965	0.965	0.993	0.706
Gasperini (2001)	1.602	1.056	0.808	0.900	0.966	0.765	0.825	0.931	1.643
Albarelo and D'Amico (2004)	1.821	1.189	1.365	1.723	0.813	1.083	1.065	1.045	0.759
Gómez (2006)	1.620	1.232	0.981	1.002	0.860	0.884	0.949	0.948	0.707
Faccioli and Cauzzi (2006)	1.004	1.166	1.024	1.228	0.797	0.883	1.151	1.176	1.752

derived for application in cases where the fault dimensions are unknown. This relation is based on a point source assumption and gives the intensity as a function of epicentral distance. The GMPE are derived from an extensive dataset of macroseismic intensities for large earthquakes in the Campania region and are valid for shallow crustal earthquakes in the magnitude range  $M_w = 6.3-7.0$  and in the distance range 0–300 km. It is not recommended to extrapolate outside these validity bounds. The derived relations can provide the intensities for a future earthquake in the Campania region within one intensity unit. The similar prediction errors for a Monte Carlo approach and a standard regression indicate that the uncertainties related to the fault definition are negligible in

comparison to those associated with the individual intensity observations. The latter are of the order of one intensity unit and limit the goodness of fit obtainable using any GMPE for Italy.

**Acknowledgements** The presented work was carried out as part of the EC funded project SAFER ([www.safeproject.net](http://www.safeproject.net)). Figure 1 was drawn using the Generic Mapping Tools (GMT, Wessel and Smith 1998).

## Appendix

In the following Tables 8, 9, 10, and 11, the covariance matrices for the four regressions are presented.

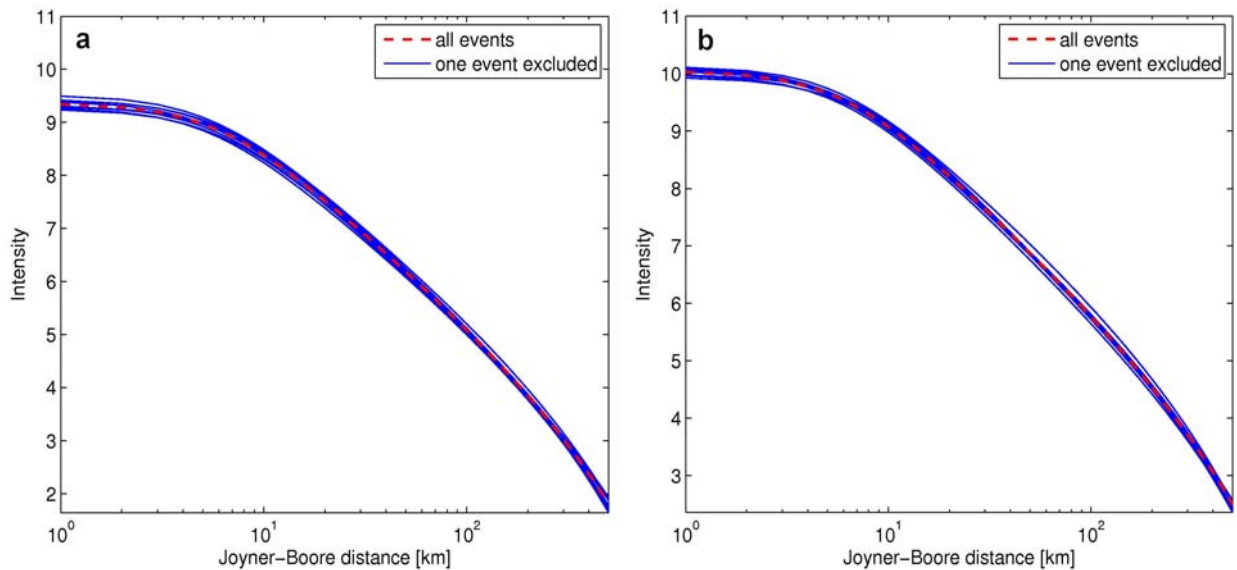


**Fig. 7** Comparison of the GMPE in Table 6 for an **a**  $M = 6.3$  earthquake and **b**  $M = 7.0$  earthquake. The relation derived from all events is marked with a red dotted line.

**Table 8** Covariance matrix for Monte Carlo regression for Joyner–Boore distance

	<i>c</i>	<i>e*</i>	<i>a</i>	<i>b</i>	<i>h*</i>
<i>c</i>	6.320e-2	-4.120e-1	-8.285e-2	2.904e-4	-3.699e-1
<i>e*</i>	-4.120e-1	2.702	5.029e-1	-1.799e-3	2.164
<i>a</i>	-8.285e-2	5.029e-1	4.537e-1	-1.423e-3	2.076
<i>b</i>	2.904e-4	-1.799e-3	-1.423e-3	4.783e-6	-6.129e-3
<i>h*</i>	-3.699e-1	2.164	2.076	-6.129e-3	1.048e+1

The diagonal elements, representing the squared uncertainties of the individual parameters, are marked as gray.

**Table 9** Covariance matrix for standard regression for Joyner–Boore distance

	<i>c</i>	<i>e*</i>	<i>a</i>	<i>b</i>	<i>h*</i>
<i>c</i>	7.060e-3	-4.747e-2	-4.366e-5	3.358e-6	9.795e-4
<i>e*</i>	-4.747e-2	3.218e-1	-1.619e-3	-1.644e-5	-2.422e-2
<i>a</i>	-4.366e-5	1.619e-3	2.186e-2	-9.331e-5	6.756e-2
<i>b</i>	3.358e-6	-1.644e-5	-9.331e-5	4.940e-7	-2.495e-4
<i>h*</i>	9.795e-4	-2.422e-2	6.756e-2	-2.495e-4	2.822e-1

The diagonal elements, representing the squared uncertainties of the individual parameters, are marked as gray.

**Table 10** Covariance matrix for Monte Carlo regression for epicentral distance

	<i>c</i>	<i>e*</i>	<i>a</i>	<i>b</i>	<i>h*</i>
<i>c</i>	9.970e-2	-6.428e-1	-8.118e-2	2.454e-4	-4.920e-1
<i>e*</i>	-6.428e-1	4.211	2.933e-1	-9.836e-4	1.827
<i>a</i>	-8.118e-2	2.933e-1	1.357	-3.586e-3	6.994
<i>b</i>	2.454e-4	-9.836e-4	-3.586e-3	9.812e-6	-1.812e-2
<i>h*</i>	-4.920e-1	1.827	6.994	-1.812e-2	3.814e+1

The diagonal elements, representing the squared uncertainties of the individual parameters, are marked as gray.

**Table 11** Covariance matrix for standard regression for epicentral distance

	<i>c</i>	<i>e*</i>	<i>a</i>	<i>b</i>	<i>h*</i>
<i>c</i>	7.001e-3	-4.645e-2	-7.920e-4	5.052e-6	-6.040e-3
<i>e*</i>	-4.645e-2	3.132e-1	4.280e-3	-9.435e-6	-2.994e-2
<i>a</i>	-7.920e-4	-4.280e-3	7.945e-2	-2.494e-4	3.133e-1
<i>b</i>	5.052e-6	-9.435e-6	-2.494e-4	8.875e-7	-8.816e-4
<i>h*</i>	-6.040e-3	-2.994e-2	3.133e-1	-8.816e-4	1.566

The diagonal elements, representing the squared uncertainties of the individual parameters, are marked as gray.

## References

- Albarelo D, D’Amico V (2004) Attenuation relationship of macroseismic intensity in Italy for probabilistic seismic hazard assessment. *Boll Geofis Teor Appl* 45(4):271–284
- Berardi R, Petruccaro C, Zonetti L, Magri L, Mucciarelli M (1993) *Mappe di sismicità per l’area italiana*, ISMES/ENEL, 51 pp
- Boschi E, Ferrari G, Gasperini P, Guidoboni E, Smriglio G, Valensise G (1995) *Catalogo dei forti terremoti in Italia dal 461 A.C. al 1980*. ING-SGA, Bologna
- Canciani A (1904) Sur l’emploi d’une double échelle sismique des intensités empirique et absolute. In: Rudolph E (ed) *Verhandlungen der vom 24–28. Juli 1903 zu Strassburg abgehaltenen zweiten internationalen seismologischen Konferenz*. Gerlands Beitr Geophys Suppl II:281–283
- CNR-PFG (1985) *Atlas of isoseismal maps of Italian earthquakes*, Quad Ric Scient, Pubbl. 114
- Dziewonski AM, Ekström G, Franzen JE, Woodhouse JH (1988) Global seismicity of 1980: centroid-moment tensor solutions for 515 earthquakes. *Phys Earth Planet Inter* 50:127–154. doi: 10.1016/0031-9201(88)90003-9
- Emolo A, Iannaccone G, Zollo A, Gorini A (2004) Influences on the source mechanisms of the 1930 Irpinia (Southern Italy) earthquake from simulations of the kinematic rupture

- process. *Ann Geophys* 47(6): 1743–1754
- Faccioli E, Cauzzi C (2006) Macroseismic intensities for seismic scenarios, estimated from instrumentally based correlations. In: Proceedings of the first European conference on earthquake engineering and seismology, Geneva, Switzerland, 3–8 September, Paper no. 569
- Gasparini P (2001) The attenuation of seismic intensity in Italy: a bilinear shape indicates the dominance of deep phases at epicentral distances longer than 45 km. *Bull Seismol Soc Am* 91(4):826–841. doi: 10.1785/0120000066
- Gasparini P, Bernardini F, Valensise G, Boschi E (1999) Defining seismogenic sources from historical earthquake felt reports. *Bull Seismol Soc Am* 89(1):94–110
- Gómez AA (2006) Seismic hazard map for the Italian territory using macroseismic data. *Earth Sci Res J* 10(2):67–90
- Grünthal G (ed) (1998) European macroseismic scale 1998 (EMS-98). *Cahiers du Centre Européen de Géodynamique et de Séismologie*, vol. 15, Luxembourg, 99 pp
- Gruppo di lavoro CPTI (2004) Catalogo Parametrico dei Terremoti Italiani, versione 2004 (CPTI04), INGV, Bologna. <http://emidius.mi.ingv.it/CPTI04/>
- Jánosi I (1907) Bearbeitung der makroseismischen Erdbeben auf Grund der “Cancanischen Gleichung”, Technical report, K. u. K. Reichsanstalt für Meteorologie u. Erdmagnetismus, Budapest
- Joyner WB, Boore DM (1993) Methods for regression analysis of strong-motion data. *Bull Seismol Soc Am* 83(2):469–487
- Kárník V (1969) Seismicity of the European area. Kluwer, Dordrecht
- Kövesligethy R (1906) A makroseismikus renesek feldolgozása. *Mathematikai és Természettudományi Értesítő* 24:349–368
- Oddone E (1930) Studio sul terremoto avvenuto il 23 luglio 1930 nell’Irpinia, Relazione a S.E. il Ministro dell’Agricoltura e Foreste, in *La meteorologica practica*, Regio Ufficio centrale di Meteorologica e Geofisica
- Postpischl D (ed) (1985) *Catalogo dei terremoti Italiani dall’anno 1000 al 1980*, CNR, P.F. Geodinamica, Graficop Bologna (1985), 239 pp
- Sørensen MB, Stromeyer D, Grünthal G (2009) Attenuation of macroseismic intensity - new relation for the Marmara Sea region, NW Turkey. *Bull Seismol Soc Am* 99(2A):538–553
- Sponheuer W (1960) *Methoden zur Herdtiefenbestimmung in der Makroseismik*, Freiburger Forschungsh. C88, 120 pp
- Stromeyer D, Grünthal G, Wahlström R (2004) Chi-square regression for seismic strength parameter relations, and their uncertainties, with applications to an  $M_w$  based earthquake catalogue for central, northern and north-western Europe. *J Seismol* 8:143–153. doi: 10.1023/B:JOSE.0000009503.80673.51
- Stromeyer D, Grünthal G (2009) Attenuation relationship of macroseismic intensities in Central Europe. *Bull Seismol Soc Am* 99(2A):554–565
- Stucchi M, Camassi R, Rovida A, Locati M, Ercolani E, Meletti C, Migliavacca P, Bernardini F, Azzaro R (2007) DBMI04, il database delle osservazioni macrosismiche dei terremoti italiani utilizzate per la compilazione del catalogo parametrico CPTI04. <http://emidius.mi.ingv.it/DBMI04/>, *Quaderni di Geofisica*, vol. 49
- Weber E, Convertito V, Iannaccone G, Zollo A, Bobbio A, Cantore L, Corciulo M, Di Crosta M, Elia L, Martino C, Romeo A, Satriano C (2007) An advanced seismic network in the Southern Apennines (Italy) for seismicity investigations and experimentation with earthquake early warning. *Seismol Res Lett* 78:622–634. doi: 10.1785/gssrl.78.6.622
- Wells DL, Coppersmith LJ (1994) New empirical relationships among magnitude, rupture length, rupture width, rupture area, and surface displacement. *Bull Seismol Soc Am* 84(4):974–1002
- Wessel P, Smith WHF (1998) New improved version of Generic Mapping Tools released. *EOS* 79:579. doi:10.1029/98EO00426